A novel method for analyzing formalin-fixed paraffin embedded (FFPE) tissue sections by mass spectrometry imaging

By Yutaka AOKI,[*1,*2] Atsuhiko TOYAMA,[*1,*2] Takashi SHIMADA,[*1,*2] Tetsuyoshi SUGITA,[*1,*2] Chikage AOKI,[*1,*2] Yukari UMINO,[*1,*2] Atsushi SUZUKI,[*3] Daisuke AOKI,[*3] Yataro DAIGO,[*2] Yusuke NAKAMURA[*4] and Taka-Aki SATO[*1,*2,†]

(Communicated by Koichi TANAKA, M.J.A.)

Abstract: Significant advances have been made in the past decade in the field of mass spectrometry imaging (MS imaging). It is a relatively unestablished technique aimed at direct, high-sensitive and spatially exclusive detection of biological molecules from the surface of tissue sections, so that semi-quantitative distribution map of the analyte can be reconstituted from the mass spectra obtained. There is tremendous potential in its application especially in clinical field, such as biomarker discovery or pharmacokinetic study. However, vast majority of the work has been performed on frozen tissue sections, while it remains generally unpractical to produce frozen sections with clinically resected tumor samples. Here we report our novel sample preparation technique that enabled MS imaging from formalin-fixed paraffin embedded (FFPE) tissue section, including retrospective archive as old as 11 years. FFPE sections were first dewaxed with pre-warmed xylene, and exposed tissue surface was enzymatically digested in nanoliter scale droplets to retain analyte localization. As a result, we succeeded in obtaining MS images of peptide peaks derived from several proteins, identified by MS/MS analysis, using ovarian cancer FFPE sections. The qualities of mass spectra obtained by this method were not significantly different from those obtained from frozen sections. By this, we opened the door to retrospective study of past clinical cases in aim to discover molecular biomarker.

Keywords: matrix-assisted laser desorption/ionization time-of-flight mass spectrometry, mass spectrometry imaging, formalin-fixed paraffin embedded, ovarian cancer

1. Introduction

Imaging by matrix-assisted laser desorption/ionization mass spectrometry (MALDI-TOF MS)[1] using tissue samples is a relatively new technique that is specialized for direct analysis of localized protein expression at microscopic spatial resolution, which is hoped to add another dimension to the current field of proteomic analysis.[2] It offers a potential solution for visually bridging histopathological study of tissues to structural and expressional study of proteins, which is especially important for cancer research and biomarker validation.[3] Indeed, investigation on MS-compatible staining methods[4] and attempts to associate MS imaging with immunohistochemistry[5] have been recently reported as foundational studies. However, all publications to date use freshly prepared frozen tissue sections and no success has been reported with regard to formalin-fixed paraffin embedded (FFPE) tissue sections that hold even greater clinical potential. Using FFPE samples for clinical

[*1] Life Science Laboratory, Shimadzu Corporation, Kyoto 604-8511, Japan.
[*2] Division of Advanced Clinical Proteomics, Institute of Medical Science, University of Tokyo, Tokyo 108-8639, Japan.
[*3] Department of Obstetrics and Gynecology, Keio University School of Medicine, Tokyo 160-8582, Japan.
[*4] Laboratory of Molecular Medicine, Human Genome Center, Institute of Medical Science, University of Tokyo, Tokyo 108-8639, Japan.
[†] Corresponding should be addressed: Taka-Aki Sato, Proteomics Research Center, Shimadzu Corporation, 3-17-1, Azuma, Tsukuba 305-0031, Japan
(e-mail: takaaki@shimadzu.co.jp).

Abbreviations: CHIP: Chemical Inkjet Printer; CSV: comma separated value; DHB: 2,5-dihydroxybenzoic acid; ESI: electrospray ionization; FFPE: formalin-fixed paraffin embedded; ITO: indium tin oxide; LC: liquid chromatography; MALDI-TOF: matrix-assisted laser desorption/ionization time-of-flight; MS: mass spectrometry; OCT: optimal cutting temperature; PBS: Phosphate-buffered saline; SA: sinapinic acid.

doi: 10.2183/pjab/83.205

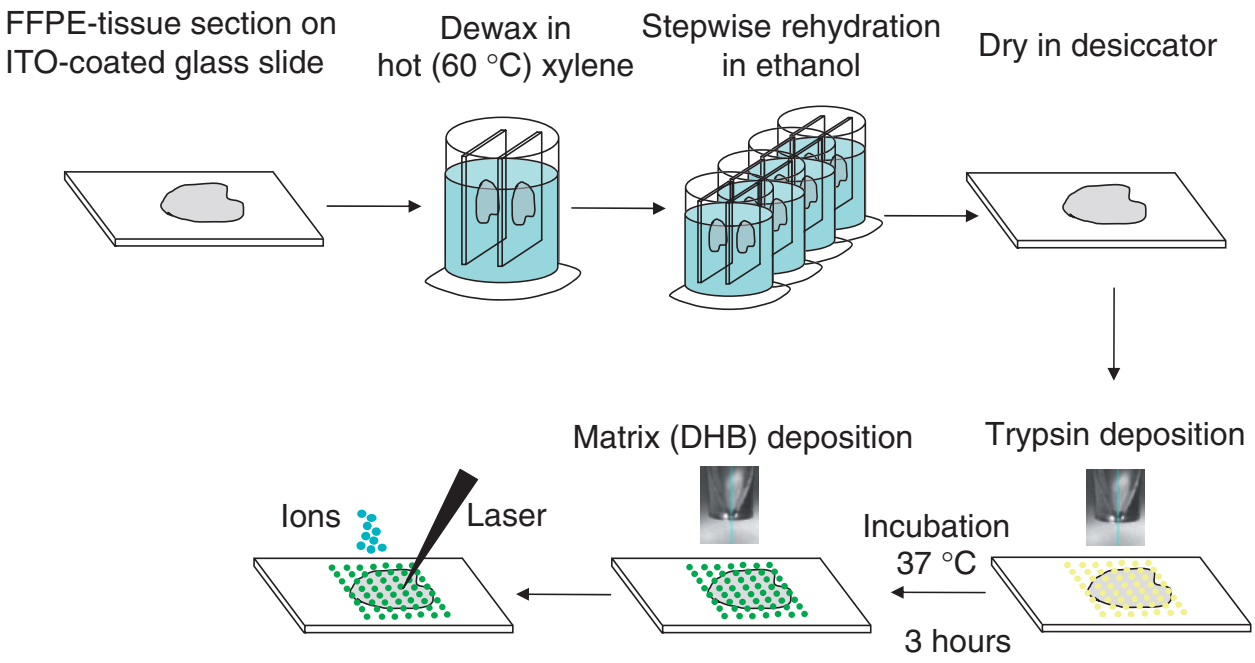

Fig. 1. FFPE tissue sections require rigorous dewaxing followed by in-situ enzymatic digestion and MALDI matrix deposition for direct MALDI-TOF MS analysis. FFPE tissue section mounted on indium tin oxide (ITO)-coated glass slide was dewaxed by gently immersing the section for 10 minutes in 100% xylene, which was kept at 60 °C for efficient paraffin solvation. After rehydration, exposed tissue surface was enzymatically digested by depositing nano-droplets of trypsin by chemical inkjet printer (CHIP-1000). After 3-hour incubation at 37 °C, MALDI matrix was similarly deposited to prevent diffusion of peptides.

research would overcome three difficulties encountered by other biological samples (e.g., serum): first, tremendous time and cost needed to accumulate enough sample numbers is alleviated; second, the sampling and storage protocol is already well-established; and finally, the follow-up studies have already been performed for each sample to link result with clinical outcomes. There are archives of FFPE samples worldwide waiting to be analyzed, not only in clinical field but also in plant and insect biology because it is difficult to preserve plants and insects in frozen form.

Therefore we aimed solely at acquiring valid MS images using FFPE sections that are comparable to those obtained from frozen sections, and this is the first report that describes the sample preparation techniques needed for MS imaging of FFPE tissue, as summarized in Fig. 1. Not surprising from its semi-permanent stability, proteomic analysis of FFPE sections are indeed challenging because of embedding paraffin and chemical cross-linking of formaldehyde.

We developed a novel sample preparation technique that incorporates the modified dewaxation protocol and in-situ tryptic digestion within nanoliter scale droplets by chemical inkjet printer to retain analyte localization.[6] MALDI matrix was applied in the same fashion to ensure the formation of uniform crystals, a critical factor for reproducible signal acquisition.[7),8]

Using this technique, we first analyzed and compared the mass spectra acquired from frozen and FFPE tissue sections of the same sample source, and demonstrated that observed peptide signals were of equivalent quality in both samples. Critically, we demonstrated that this sample preparation technique can be applied to retrospective analysis of old (11 years old) samples to obtain sufficient signals for MS imaging, pioneering the field of retrospective MS imaging study.

2. Materials and methods

Reagents. Bradykinin fragment 1-7, used for peptide standard and ITO-coated glass slides, 8-12 ohms, were purchased from Sigma-Aldrich (St. Louis, MO). Sequencing grade modified trypsin

was purchased from Promega (Madison, WI). All other chemical reagents, including the MALDI matrices 2,5-dihydroxybenzoic acid (DHB) and sinapinic acid (SA), were purchased from Wako Pure Chemical Industry (Osaka, Japan) unless otherwise stated.

Animals. C57/B6J mice were purchased from CLEA Japan (Tokyo, Japan), sacrificed at 7 weeks of age by cervical dislocation after anesthesia under diethyl ether. The brain was removed after head incision. The brain immediately rinsed with PBS.

FFPE sample preparation. Mouse brain was fixed by immersing in Mildform 10N at room temperature for 5 hours. Fixed brain was washed under running water for 30 minutes and embedded in paraffin by automated protocol using Tissue-Tek Rotary Tissue Processor (Sakura Finetek Japan). FFPE tissue block was sliced into 10 µm sections by microtome (MICROM International), attached to ITO-coated glass slides by scooping the sections in 50 °C water bath, and dried on an extender at 45 °C. FFPE sections were dewaxed by gently immersing in xylene for 10 minutes pre-warmed to specified temperature in water bath. The slide was then washed in stepwise immersion, 5 minutes duration each, into 100% ethanol twice, 90% ethanol, 80% ethanol and finally in 70% ethanol.

Frozen tissue sample preparation. Mouse brain was embedded in optimal cutting temperature (OCT) compound and frozen to −30 °C. The frozen tissue block was sliced into 10 µm sections by cryostat microtome (Leica Microsystems) at −20 °C and attached onto ITO-coated glass slide. The section was air-dried for 1 hour and washed briefly in PBS, then in 70% ethanol, to remove OCT.

Cancer tissue samples. Ovarian cancer and endometrial cancer FFPE tissue sections were provided by Keio University with informed consent and under authorization of the ethical committees of Keio University and Institute of Medical Science, University of Tokyo.

Tryptic digestion. Sample slide was slotted into MALDI target plate, affixed with conducting tape, and inserted into chemical inkjet printer CHIP-1000 (Shimadzu Corporation). Trypsin solution was prepared by dissolving 100 µg of trypsin in 1 ml of 10 mM NH_4HCO_3 solution. Using CHIP-1000, trypsin solution was spotted over the tissue section in 2.5 nl droplets at spatial interval of 200 µm over 2 cycles. After spotting, the MALDI plate was immediately incubated at 37 °C in total humidity for 3 hours.

Matrix deposition. DHB solution was prepared at concentration of 50 mg/ml, dissolved in 50:50 acetonitrile and 0.1% trifluoroacetic acid with pre-dissolved 1 nmol/ml bradykinin fragment as internal standard. SA solution was prepared similarly at 20 mg/ml concentration. As above, CHIP-1000 was used to deposit DHB solution over digested tissue section in 0.5 nl droplets over 15 cycles at spatial interval ranging from 100 to 200 µm as will be discussed. For non-digested samples, SA solution was spotted in 1 nl droplets over 10 cycles at 200 µm interval.

Evaluation of signal acquisition. AXIMA-QIT (Shimadzu Corporation) was used for measurement of digested sections. In optimization experiments, mass spectra were automatically accumulated over 100 points at 50 µm spacing, covering the area of 450 µm square, while keeping all instrument parameters constant throughout. Peaks were harvested from each spectrum and its number was recorded, as it would numerically reflect the efficacy of signal acquisition.

Data acquisition for imaging MS analysis. After determining the optimum sample preparation procedure, MS data was acquired for molecular imaging purpose under following conditions: 50 laser shots per point; 2115 points at 100 µm spacing, covering the tissue area of 4400 µm by 4600 µm; and each laser-shot profile was stored individually in an automated fashion. The obtained collection of mass spectra was converted, for selected m/z value, into comma separated values (CSV) associating signal intensity with XY coordinate. The intensity values were normalized as the fraction of bradykinin peak intensity in the same spectrum. The resultant CSV file was graphically represented by Graph-R software (freeware produced by Toru Itoh, http://www.vector.co.jp/vpack/browse/person/an020638.html), to visualize variation of intensity over XY coordinate for selected m/z value.

3. Results

Optimization of dewaxing protocol. In order to analyze FFPE tissue sections by MALDI-TOF MS, the primary requirement was removal of

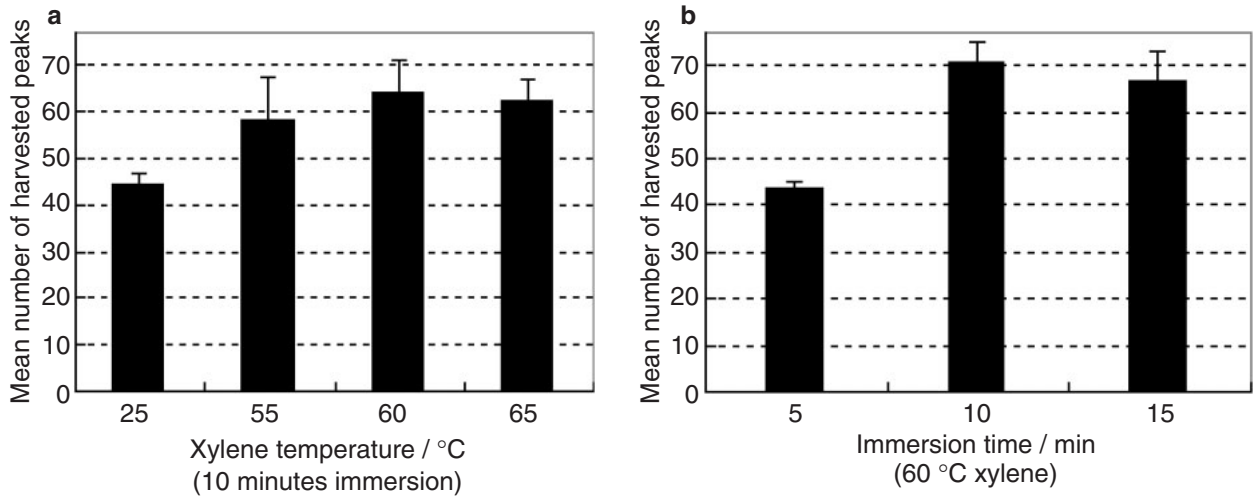

Fig. 2. The number of peaks obtained from automatic MS acquisition was plotted against various conditions to evaluate the effect of xylene temperature (a), and duration of xylene immersion (b). Best result was obtained for xylene temperature of 60 °C and 10 minutes immersion. In comparison to conventional method, increasing the temperature and immersion time significantly improves the efficacy of subsequent MS analysis ($P = 5 \times 10^{-5}$ and $P = 1 \times 10^{-6}$, respectively). Each experiment was conducted 3 times, with error bars representing standard deviation.

paraffin that would otherwise physically interfere with tryptic digestion, matrix crystallization and hence signal acquisition. First, we adhered to the conventional dewaxing procedure, that is, three sequential immersion of tissue slide in 100% xylene for 5 minutes at room temperature. However, it appeared that there was still significant amount of residual paraffin on the tissue, and the resultant signal obtained was not satisfactory. To improve the dewaxing protocol, we investigated two factors; temperature and immersion time of xylene. The efficacy of dewaxing protocol was evaluated by taking the final number of harvested peaks as a numerical indicator of general quality of MALDI-TOF MS analysis. Fig. 2 represents the graphical representation of the result ($n = 3$), showing improvement in signal acquisition, due to more efficient paraffin removal, when pre-warmed xylene was used ($P = 5 \times 10^{-5}$) and for immersion time of 10 minutes or longer ($P = 1 \times 10^{-6}$). Therefore, for all following experiments, we fixed the dewaxing protocol by 60 °C pre-warmed xylene and 10 minutes immersion time.

Effect of enzymatic digestion. Not unexpectedly, we demonstrated that direct MALDI-TOF MS analysis of intact FFPE sections by conventional methods (measuring high molecular weight ions by linear mode using SA as matrix) was totally inadequate, even after appropriate dewaxing step. Virtually no protein signal was detected from FFPE sections whereas numerous peaks were obtained from frozen sections of the same origin (Fig. 3). By direct enzymatic digestion of the tissue, we succeeded in acquisition of adequate mass spectra from FFPE sections with peptide peaks that can be identified by MS/MS analysis. The comparison of peak profiles obtained from frozen and FFPE sections revealed that 26 peaks (about 20% of total peaks) were observed in both spectra. One such peak with m/z 1274.6 was analyzed by MS/MS by AXIMA-QIT to identify the peptides by *de novo* amino acid sequencing and yielded the same result from both spectra, suggesting that unmodified peptide fragment can be recovered from formalin-fixed proteins by enzymatic digestion. In order to show that spectra obtained from FFPE samples are as applicable to MS imaging as frozen sections, the quality of spectra was evaluated by total peak numbers and normalized peak intensities of three common peaks. The difference between the total peak numbers was not significant and individual peak intensities can be even greater compared to those obtained from frozen sections.

Micro-spotting of DHB results in formation of uniform crystals. Although DHB is the optimum matrix for AXIMA-QIT to perform MS/MS

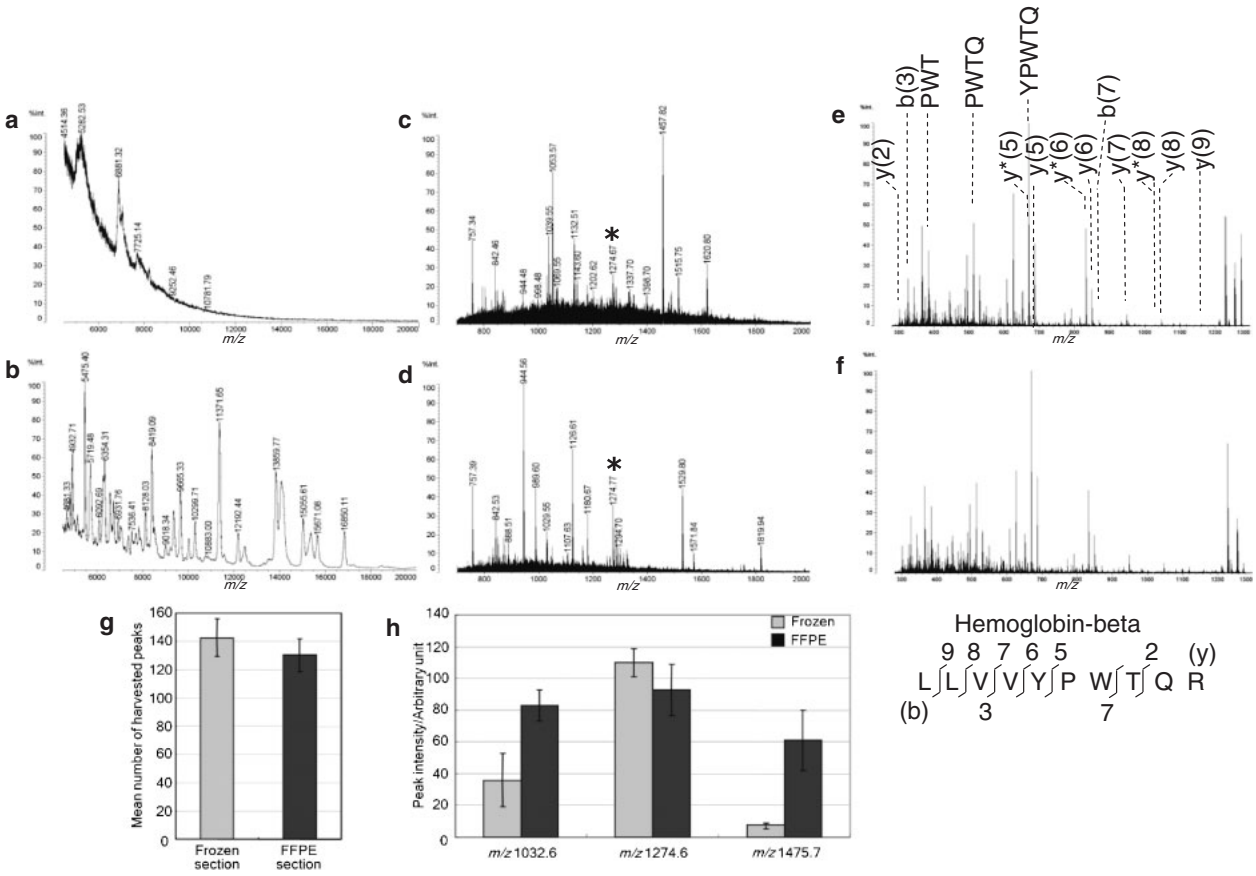

Fig. 3. (a, c and e) Mass spectra acquired from dewaxed FFPE sections. (b, d and f) Corresponding counterpart acquired from frozen sections. (a-b) Mass spectra before trypsin digestion, using sinapinic acid as matrix. No effective signal was obtained from FFPE section (a), contrasted by numerous peaks from frozen section (b). (c-d) Mass spectra of in-situ digested FFPE (c) and frozen (d) tissue sections. The peak marked with an asterisk ($m/z = 1274.6$) was further analyzed by MS/MS, giving the juxtaposed spectra (e-f, respectively). (g-h) The quality of spectra was evaluated by comparing the total number of peaks and normalized peak intensities of three common peaks. The results shown are representative of 3 experiments and error bars represent standard deviation.

analysis of excellent sensitivity, it was regarded unsuitable for MS imaging as it forms uneven, needle crystals that concentrate analytes into random, confined area commonly known as "sweet spots". To overcome this problem, we spotted highly concentrated solution of DHB in nano-scale droplets by using a chemical inkjet printer CHIP-1000. We investigated the effect of spatial interval of individual spots ranging from 100 µm to 200 µm (n = 3). Efficacy of MS measurement was evaluated by peak numbers as previously discussed, and the results were summarized in Fig. 4, together with the picture showing general appearance of the DHB microcrystals. As a result, we observed that 150 µm or 175 µm spacing resulted in the best outcome. However, optimal spatial interval of matrix spotting can change depending on matrix and solvent composition, and should be empirically assigned.

MS imaging of FFPE ovarian tumor section. FFPE ovarian tumor section was prepared for direct MS analysis by optimized paraffin removal and direct trypsin digestion. Non-cumulative MS data was acquired for MS imaging and the data was processed as described in materials and methods section. Fig. 5 shows the MS images of three representative peptide peaks, identified as hemoglobin, actin alpha-1 and ATP synthase beta-chain. The images of actin and ATP synthase showed a clear overlap with the tissue section outline, which is not surprising since both proteins are major

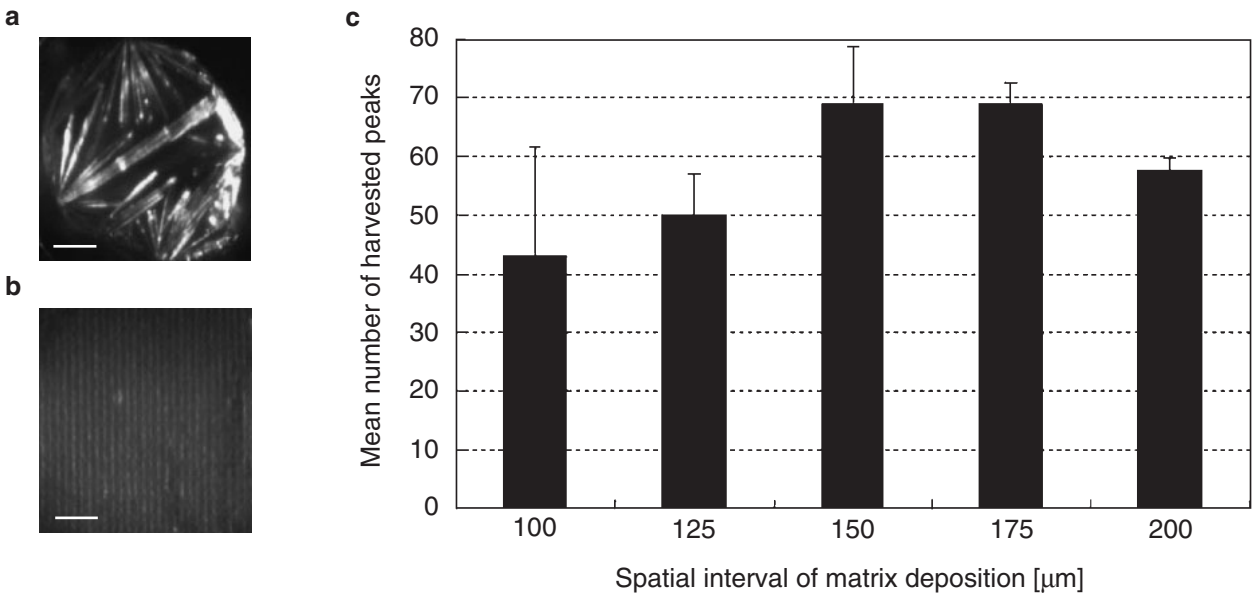

Fig. 4. (a) Appearance of typical DHB crystals formed by manually spotting 1 μl of DHB solution onto a target plate. (b) Appearance of uniform DHB microcrystals formed by using CHIP-1000 to deposit 0.5 nl of concentrated DHB solution into an array. (c) Histogram showing the effect of spatial interval of matrix deposition on MS acquisition (n = 3). Large error bars of standard deviation reflect the reproducibility of acquisition. When deposition spacing was too small, matrix droplets tended to merge, giving larger, less uniform crystals. Scale bars represent 1 mm each.

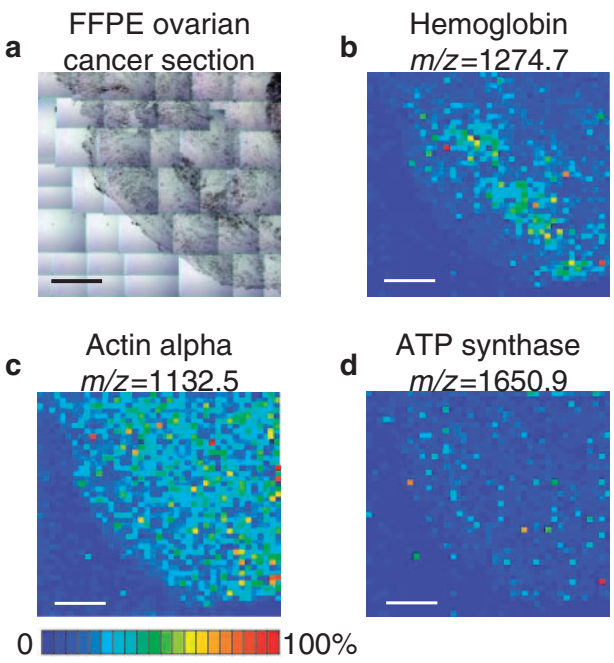

Fig. 5. (a) Bright-field micrograph of FFPE ovarian cancer section before matrix deposition, and three representative MS images acquired from this section are shown; hemoglobin (b), actin alpha (c) and ATP synthase (d). Scale bars represent 1 mm each.

house-keeping proteins and are not expected to specifically localize. In contrast, the hemoglobin image showed a strongly localized pattern. MS/MS measurements were performed on other prominent peaks, and 39 out of 58 peaks were successfully identified, as listed in Table 1. One of the identified peptide was derived from N-terminus of the original protein, which was modified by N-terminal acetylation (data not shown).

Retrospective analysis of endometrial cancer. We analyzed groups of 1 month- and 11 years-old FFPE endometrial cancer sections by MALDI-TOF MS and compared the spectra obtained from non-cancer regions under the same conditions (Fig. 6). The signal attainability was assessed by total number of peaks and normalized peak intensities of four representative peaks (derived from actin beta as identified by MS/MS). As a result, we observed slight but significant ($P = 0.005$) decrease in the number of harvested peaks in 11 years-old section, from 130.0 to 111.8 on average. Normalized signal intensities of individual peaks also show marked decrease form 1 month to 11 years, though alterations in peak profiles are expected from samples of different individuals.

Table 1. List of peptide peaks that were confidently identified by MS/MS analysis from FFPE human ovarian cancer section

observed m/z	Sequence	Protein name
660.07	—	<no match>
788.43	—	<no match>
805.52	—	<no match>
870.50	—	<no match>
944.51	R.AGLQFPVGR.V	histone cluster 1, H2ab
976.45	K.AGFAGDDAPR.A	actin, beta
1002.57	R.LMHLEFGR.G	collagen, type VI, alpha 3
1032.58	K.IRPFFPQQ.-	fibrinogen beta chain
1071.57	R.MFLSFPTTK.T	hemoglobin, alpha 2
1082.52	R.VSEEWYNR.L	collagen, type XIV, alpha 1 (undulin)
1103.53	—	<no match>
1180.63	R.ISGLIYEETR.G	histone cluster 2, H4a
1130.57	R.GYSFVTTAER.E	actin, alpha 2, smooth muscle, aorta
1132.56	R.GYSFTTTAER.E	actin, beta
1151.60	R.FTNIGPDTMR.V	fibronectin 1
1180.67	R.ISGLIYEETR.G	histone cluster 2, H4a
1198.66	R.AVFPSIVGRPR.H	actin, gamma 2, smooth muscle, enteric
1212.61	R.VNHFVPEAGSR.L	collagen, type VI, alpha 3
1231.35	—	<no match>
1250.63	R.DQLLPPSPNNR.I	collagen, type VI, alpha 1
1287.71	M.PMFIVNTNVPR.A	macrophage migration inhibitory factor
1314.66	K.VNVDEVGGEALGR.L	hemoglobin, beta
1323.69	R.EEAENTLQSFR.Q	vimentin
1325.71	L.SGGTTMYPGIADR.M	actin, gamma 1
1348.67	—	<no match>
1357.73	K.IAWESPQGQVSR.Y	fibronectin 1
1365.71	—	<no match>
1366.73	—	<no match>
1378.70	—	<no match>
1400.78	—	<no match>
1429.74	K.AFGPGLQGGSAGSPAR.F	filamin A, alpha (actin binding protein 280)
1432.76	—	<no match>
1460.69	—	<no match>
1467.81	R.RHPDYSVVLLLR.L	albumin
1490.72	—	<no match>
1520.72	R.LDALQAAAARLDHR.R	NHS-like 1
1521.91	—	<no match>
1529.86	K.VGAHAGEYGAEALER.H	hemoglobin, alpha 2
1565.78	R.VDAQDETAAEFTLR.L	elastin microfibril interfacer 1
1623.79	K.DVFLGMFLYEYAR.R	albumin
1624.81	R.TGAIVDVPVGEELLGR.V	ATP synthase, alpha subunit 1
1634.74	—	<no match>
1640.80	—	<no match>
1646.85	R.DVWGIEGPIDAAFTR.I	vitronectin
1743.91	K.AMGIMNSFVNDIFER.I	histone cluster 1, H2bo
1763.78	K.LISWYDNEFGYSNR.V	glyceraldehyde-3-phosphate dehydrogenase
1775.99	—	<no match>
1790.82	K.SYELPDGQVITIGNER.F	actin, beta

Continued on the next page.

Continued.

observed m/z	Sequence	Protein name
1823.89	Y.ANTVLSGGTTMYPGIADR.M	actin, gamma 1
1912.96	R.SSPVVIDASTAIDAPSNLR.F	fibronectin 1
1836.86	R.DGQVINETSQHHDDLE.-	vimentin
1926.02	R.VTWAPPPSIDLTNFLVR.Y	fibronectin 1
1953.98	R.VAPEEHPVLLTEAPLNPK.A	actin, beta
2141.00	R.GTELGGAAGQGGHPPGYTSLASR.L	elastin microfibril interfacer 1
2193.97	R.YGGLHFSDQVEVFSPPGSDR.A	collagen, type VI, alpha 2
2215.04	K.DLYANTVLSGGTTMYPGIADR.M	actin, gamma 1
2283.22	R.AIPHPAYNPKNFSNDIMLLQ.L	granzyme B
2576.31	—	<no match>

4. Discussion

The nature of FFPE tissues has long been imposing a great limitation to its proteomic analysis, primarily because of the extensive crosslinks induced by formaldehyde fixation. The randomness and irreversibility of the inter-protein crosslinks have made intact protein separation impossible, as demonstrated by comparative two-dimensional gel electrophoresis analysis where protein extracted from FFPE tissue resulted in no spot, contrasted by efficient protein retrieval from ethanol fixation.[9] The only feasible proteomic analysis method for FFPE tissues so far is described by Hood et al., who used reverse phase LC linked to ESI-MS/MS for shotgun identification of enzymatically digested peptides.[10] It can be modeled that proportion of each protein can be retrieved by digesting across the crosslinked structure because conventional formaldehyde fixation does not affect all potential attacking sites.

Our reporting MS analysis of FFPE tissue sections followed the same bottom-up principle, and we have acquired peptide signals from FFPE sections that were equivalent to those of frozen sections in signal intensity and diversity. Critically, none of the MS/MS spectra showed any sign of formaldehyde derivative, which should be the case if formaldehyde attacks result in crosslink to other surrounding molecules. Moreover, only 2 of 42 peptides were of missed cleavages, indicating that trypsin digestion condition was generally favorable and could digest across crosslinked structure of proteins.[11] Therefore we conclude that our modified dewaxation, in-situ digestion and matrix deposition protocols made paraffin embedment no longer an inhibitory factor to ionization of peptides for MS imaging analysis. Moreover, this technique can potentially be applied to analysis of other biological molecules by the same principle, such as lipids, metabolites and oligonucleotides, although strategies to overcome formaldehyde fixation needs consideration for each type of analysis. For example, it should be possible to monitor the effect of drug introduction by directly detecting fluctuation in low molecular weight metabolites, including the drug compound itself and its biochemical derivatives. Above all, the most critical application of this technique is for retrospective studies using sample archives. However, in this report we have failed to show that equivalent signal yield can be acquired regardless of the time of FFPE preparation, even though the signal yield was good enough for MS imaging by itself. It appeared that signal intensities of the same peak profile had generally deteriorated in old sections, possibly because of long-term sample degradation, as frequently experienced in immunohistochemistry as well. If this phenomenon is solely attributable to non-specific degradation, we should be able to acquire the same peak profiles by applying appropriate normalization.

The dynamic range of MS imaging analysis is admittedly still underdeveloped, since we only managed to identify cytoskeletal proteins, globins and house-keeping proteins that are most abundantly present in tissues. This is largely attributable to the methodology itself. Even with standard samples, the dynamic range of detection of MALDI-TOF MS instrument will not exceed three orders of magnitude[12] due to factors such as detector satu-

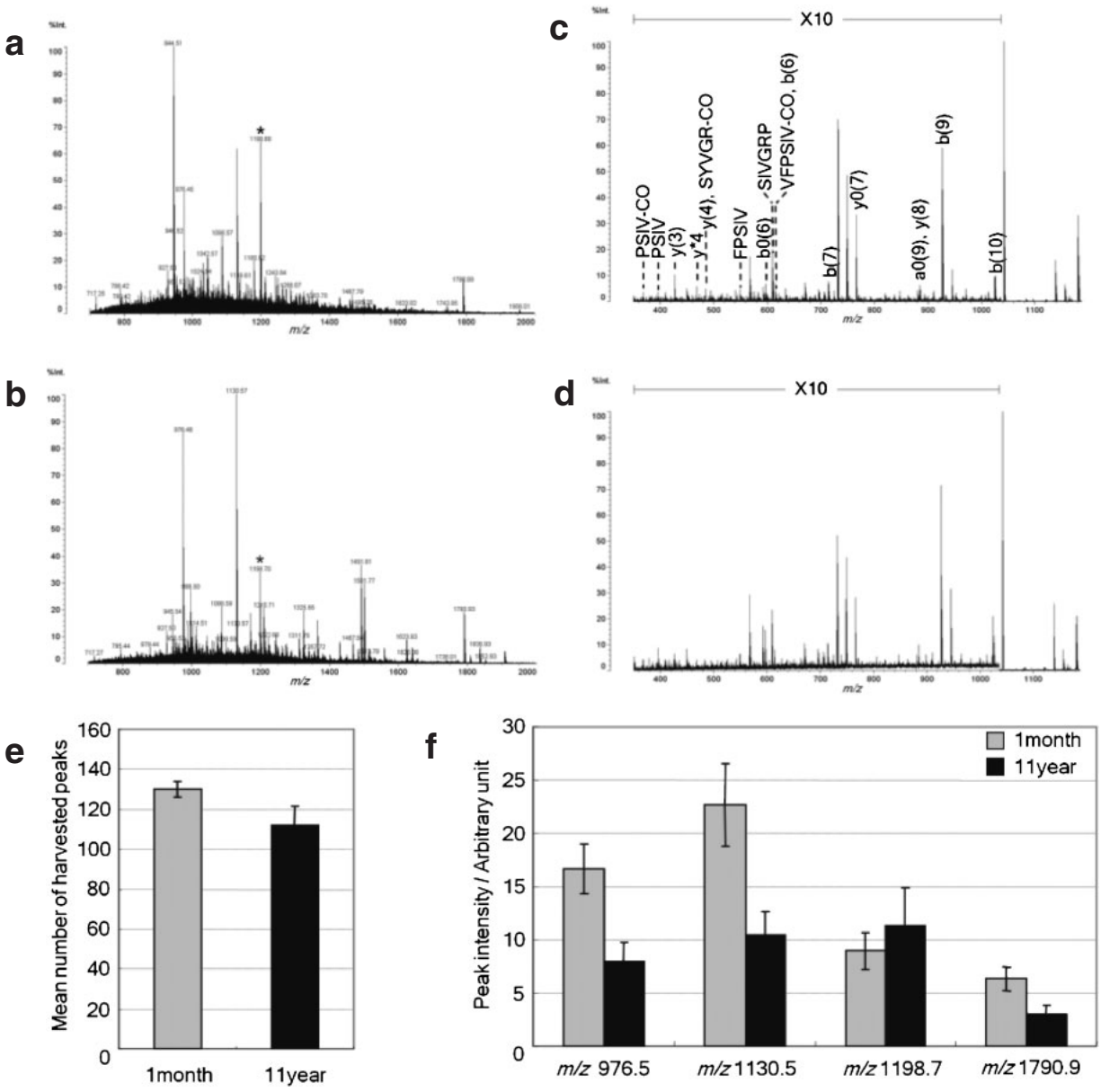

Fig. 6. Mass spectra obtained from 1 month-old (a) and 11 years-old (b) FFPE endometrial cancer sections, juxtaposed by corresponding MS/MS spectra of m/z 1198.7 (c-d, respectively). (e-f) The quality of spectra was evaluated by comparing the total number of peaks and normalized peak intensities of four peaks derived from actin beta. The results shown are representative of 5 experiments and the error bars represent standard deviation.

ration, uneven surface, and ion suppression by analytes of higher abundance. LC-MS/MS strategy has advantage over MALDI-TOF MS-based strategy in this respect, as it involves pre-separation of peptides that reduces the number of peptide species being analyzed simultaneously. However, tumor markers, especially those detected at tissue surface, are not necessarily low abundant proteins. In deed, there are clinically used biomarkers that are heavily overexpressed such as keratin-19 of lung squamous cell carcinoma.[13] It should be emphasized that MS imaging is a more research-directed technique compared to the discovery-driven nature of shotgun approach, as MS imaging gives both spatial and

quantitative data that can be directly associated with conventional analysis such as immunohistochemistry.[14] By world-wide comprehensive research, which is a realistic prospect considering the archive of samples stored, it is hoped that the technique described here will contribute to the discovery of subtle but statistically affirmed expressional change associated with carcinogenesis that could be used for tumor diagnosis and reliable prognostic prediction.

5. Acknowledgments

We greatly thank Dr. Mitsutoshi Seto (Okazaki Institute for Integrative Bioscience, National Institutes of Natural Sciences) for general discussion.

References

1) Karas, M. and Hillenkamp, F. (1988) Anal. Chem. **60**, 2299–2301.
2) Guerrera, I. C. and Kleiner, O. (2005) Biosci. Rep. **25**, 71–93.
3) Reyzer, M. L. and Caprioli, R. M. (2005) J. Proteome Res. **4**, 1138–1142.
4) Chaurand, P., Schwartz, S. A., Billheimer, D., Xu, B. J., Crecelius, A. and Caprioli, R. M. (2004) Anal. Chem. **76**, 1145–1155.
5) Chaurand, P., Sanders, M. E., Jensen, R. A. and Caprioli, R. M. (2004) Am. J. Pathol. **165**, 1057–1068.
6) Nakanishi, T. Ohtsu, I., Furuta, M., Ando, E. and Nishimura, O. (2005) J. Proteome Res. **4**, 743–747.
7) Chaurand, P. and Caprioli, R. M. (2002) Electrophoresis **23**, 3125–3135.
8) Schwartz, S. A., Reyzer, M. L. and Caprioli, R. M. (2003) J. Mass Spectrom. **38**, 699–708.
9) Ahram, M., Flaig, M. J., Gillespie, J. W., Duray, P. H., Linehan, W. M., Ornstein, D. K., Niu, S., Zhao, Y., Petricoin, E. F., 3rd and Emmert-Buck, M. R. (2003) Proteomics **3**, 413–421.
10) Hood, B. L., Darfler, M. M., Guiel, T. G., Furusato, B., Lucas, D. A., Ringeisen, B. R., Sesterhenn, I. A., Conrads, T. P., Veenstra, T. D. and Krizman, D. B. (2005) Mol. Cell Proteomics **4**, 1741–1753.
11) Hood, B. L., Conrads, T. P. and Veenstra, T. D. (2006) Proteomics **6**, 4106–4114.
12) Tholey, A., Zabet-Moghaddam, M. and Heinzle, E. (2006) Anal. Chem. **78**, 291–297.
13) Stieber, P., Hasholzner, U., Bodenmuller, H., Nagel, D., Sunder-Plassmann, L., Dienemann, H., Meier, W. and Fateh-Moghadam, A. (1993) Cancer **72**, 707–713.
14) Ramos-Vara, J. A. (2005) Vet. Pathol. **42**, 405–426.

(Received June 13, 2007; accepted Aug. 7, 2007)